

LabVIEW-based impedance biosensing system for detection of avian influenza virus

Zhang Benhua¹, Ronghui Wang², Yixiang Wang², Yanbin Li^{2*}

(1. College of Engineering, Shenyang Agriculture University, Shenyang 110866, China;

2. Department of Biological & Agricultural Engineering, University of Arkansas, Fayetteville, AR 72701, USA)

Abstract: In order to detect the multiple avian influenza viruses (AIVs) rapidly, specifically and sensitively, a LabVIEW and microelectrode array-based impedance biosensor was developed and demonstrated. A laptop with LabVIEW software was used to generate excitation signals at different frequencies with an audio card and measure the impedance of target viruses through a data acquisition card. The audio card of the laptop was used as a function generator, while a data acquisition card was used for data communication. A virtual instrument was programmed with LabVIEW to provide a platform for impedance measurement, data processing, and control. Six interdigitated microelectrodes were placed at the bottom of six wells on a microplate to form six sensors for different AIVs and controls. Then, AIV specific ligands were immobilized on the microelectrode surface to capture target viruses. To enhance the sensitivity, AIV specific aptamers conjugated gold nanoparticles and thiocyanuric acid were employed to form a network structure and used as an amplifier. Results of the measured impedance were compared with a commercial IM6 impedance analyzer, and the error was less than 5%. The developed biosensor was portable with the sensitivity and specificity for applications to on-site or in-field rapid screening of avian influenza viruses.

Keywords: biosensor, impedance detection, avian influenza virus, LabVIEW

DOI: 10.3965/j.ijabe.20160904.1704

Citation: Zhang B H, Wang R H, Wang Y X, Li Y B. LabVIEW-based impedance biosensing system for detection of avian influenza virus. *Int J Agric & Biol Eng*, 2016; 9(4): 116–122.

1 Introduction

Potential pandemic outbreak of human infection with AIV H5N1 or H7N9 can cause a serious health threat worldwide. The Highly Pathogenic Avian Influenza (HPAI) H5N1 virus, which originally emerged in Southeast Asia at late 1990's, cost the poultry industry an estimated \$10 billion between 1997 and 2008. Since

2003, there have been 398 deaths among 676 cases of human infection caused by H5N1, for a mortality rate of 59%^[1]. In late February and early March of 2013, the AIV H7N9 emerged in humans in Shanghai and surrounding provinces of China. As of May 29, 2013 there were reported 132 confirmed H7N9 infections with 37 fatalities^[2]. Rapid, sensitive and specific detection of AIVs is becoming increasingly important and urgent. The technology for diagnosing AI infections is available, such as viral culture, diagnostic test kits, RT-PCR and ELISA methods, but these tests are of some shortcomings, such as poor specificity, low sensitivity, time consuming and high costs, and require a laboratory and a highly trained technician. In a report of WHO (2006)^[3], it was pointed out that “A simple, rapid, robust and reliable test, suitable for use in the field or at the patient's bedside, is urgently needed”. Considerable effort has been directed towards the development of simple biosensors for the

Received date: 2015-01-27 **Accepted date:** 2015-10-01

Biographies: **Zhang Benhua**, PhD, Professor, research interests: intelligent agricultural machinery and equipment, Email: zbh@syau.edu.cn; **Ronghui Wang**, PhD, Research Scientist, research interests: biosensing, molecular biology, Email: rwang@uark.edu; **Yixiang Wang**, MS, Graduate Research Assistant, research interests: bioinstruments, Email: yixiangw@uark.edu.

***Corresponding author:** **Yanbin Li**, PhD, Distinguished Professor, research interests: biosensors and bioinstrumentation, microbial predictive models, quantitative risk assessment. Mailing address: 203 Engineering Hall, Fayetteville, AR 72701, USA. Tel: +1-479-575-2881, Email: yanbinli@uark.edu.

detection of AIV, such as surface plasmon resonance, quartz crystal microbalance, fluorescence, optical interferometry, imaging ellipsometry and electrochemistry^[4-9]. These developed biosensors have shown potential but are not suitable for rapid, in-field testing. Therefore, the goal of this study was to develop a portable impedance biosensing system with the sensitivity and specificity for applications to on-site or in-field rapid screening of multiple AIVs.

Impedance measurement/detection is a powerful detection method, ideal for easy integration into multi-array or microprocessor-controlled diagnostic tools and incorporation into miniaturized analytical systems. Impedance measurement/detection can be used for “in field” measurements in combination with a portable measuring unit, and can also provide real-time in situ monitoring^[10]. In recent years, with the rapid development of computer technology, the virtual instrument technology has been widely used. In this study, virtual instrumentation using LabVIEW with a laptop was employed to generate excitation signals at different frequencies with an audio card and measure the impedance of target viruses through a data acquisition card. The developed portable biosensing system with interdigitated microelectrode based microplate array and virtual instrumentation based impedance measurement platform, is suitable for real time detection of AIVs in the field.

2 Materials and methods

2.1 Materials

Inactivated AIV H5N1 was supplied by USDA APHIS Research Laboratory (Ames, IA). The selected aptamer with high affinity and specificity against AIV H5N1 surface protein was developed in our group with detailed information described in our previous study^[11]. Biotin labeled aptamer was obtained from Integrated DNA Technologies, Inc. (Coralville, IA). The sequence is 5'-Biotin-GTG TGC ATG GAT AGC ACG TAA CGG TGT AGT AGT AAC GTG CGG GTA GGA AGA AAG GGA AAT AGT TGT CGT GTT G-3'. All chemicals used in this study unless specified were purchased from Sigma-Aldrich (St. Louis, MI).

2.2 Interdigitated microelectrode and microplate

Interdigitated microelectrodes were fabricated by Institute of Semiconductor of Chinese Academy of Sciences (Beijing, China). A 100 nm thick gold layer was sputtered on a cleaned glass substrate. In order to improve the adhesion of the gold to substrate, a 10 nm thick Cr layer was deposited prior to the gold layer. The microelectrodes were then patterned by mask photolithography and metal etching processes. Figure 1 shows the interdigitated microelectrode and the array in a microplate used in the test. Six interdigitated microelectrodes were placed at the bottom of six wells on a microplate to form six sensors for different AIVs and controls.

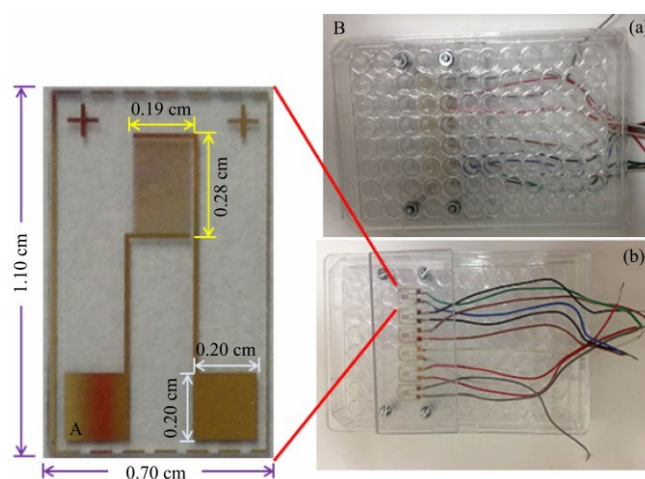


Figure 1 A: Interdigitated microelectrode; B: Microelectrode array on a microplate: (a) top view and (b) bottom view

2.2.1 Procedure

The whole experimental procedure contains four steps: electrode cleaning, surface immobilization, AI virus detection, and signal amplification. Step 1: The microelectrode was cleaned by immersing in 1 mol/L NaOH for 5 min, rinsed with deionized water, immersed in 1 mol/L HCl for 2 min, rinsed with deionized water, and then wiped gently with alcohol wetted lens paper. After final rinsing with deionized water, the microelectrode was dried with a stream of nitrogen. Step 2: The clean microelectrode was incubated with 50 μ L of streptavidin (0.5 mg/mL) at room temperature for 45 min. Following the incubation, the microelectrode was rinsed with deionized water and dried with nitrogen stream, and then incubated with 2 μ g/mL biotin-aptamer (50 μ L) for 30 min at room temperature.

After rinsing with deionized water and drying with nitrogen, the microelectrode was incubated with 0.1 mg/mL PEG (poly (ethylene glycol) methyl ether thiol) (50 μL) as a blocking solution at room temperature for 30 min. After another rinsing with deionized water and drying with nitrogen stream, the microelectrode was ready for use in detection tests. Step 3: AI detection was performed by dropping 50 μL of inactivated AI H5N1 virus onto the microelectrode surface coated with the aptamer, and incubating it at room temperature for 45 min. The impedance change caused by the target AI virus was calculated by subtracting the impedance measured at the end of step 3 from the impedance measured at the end of step 2. Step 4: 50 μL of TCA+NPApt (a conjugation of aptamer, gold nanoparticles and thiocyanuric acid) was added and incubated for 40 min at room temperature for further amplification of the signal.

2.2.2 Structure of biosensor and impedance measurement

The structure and main components of the biosensor are shown in Figure 2. Two channels sine signal with different frequencies were generated by LabVIEW through the sound card of laptop. As the signal source power, they were added to the circuit series connection of a changeless resistor R and an unknown component U (Figure 3). When the values of voltages V_1 and V_2 were tested by LabVIEW through the DAQ card, we can calculate the impedance Z of the unknown component with Equations (1) and (2).

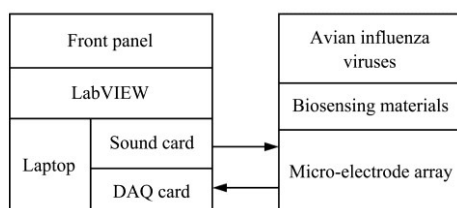


Figure 2 Structure and components of the biosensor

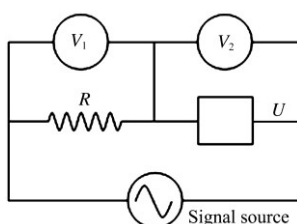


Figure 3 Circuit of impedance measurement

$$I = \frac{V_1}{R} \quad (1)$$

$$Z = \frac{V_2}{I} = \frac{V_2}{V_1 / R} \quad (2)$$

The diagram of the program based on LabVIEW is shown in Figure 4. Signal generator program is indicated in Figure 4a. In order to ensure the output signal's amplitude, a while loop of auto adjustment was designed (Figure 4b). Data acquisition and display were constructed using comprehensive library of VIs and example programs for NI LabVIEW (Figure 4c). Polymorphism Library Functions were used in this program. The front panel of the virtual instrument indicates the excitation signal, impedance recording and the final report of the detected AVIs (Figure 5).

3 Results and discussion

3.1 Principle of the biosensing of AIV

The principle of the developed biosensor is illustrated in Figure 6. Briefly, AIV specific ligands were pre-coated on the microelectrodes. The target AIVs were then captured by the immobilized ligands. To enhance the sensitivity, AIV specific aptamer was conjugated with gold nanoparticles and thiocyanuric acid in a sandwich format and then used as an amplifier (TCA+NPApt). The gold nanoparticle offered excellent electrochemical signal transduction, and thiocyanuric acid (a star-shaped trithiol molecule) was an effective capping agent for the formation of the network structure. The network-like thiocyanuric acid/gold nanoparticles can be used for signal amplification. It is due to the electrochemical oxidation/reduction of gold nanoparticles of AuCl_4^- .

3.2 Proof of the concept for AIV detection

Inactivated AI H5N1 virus with titers in the range from 2^0 to 2^5 HAU in buffer solution was tested using the developed biosensor system. Figure 7 shows the typical Nyquist diagram of impedance spectra on the bare microelectrode, streptavidin modification, aptamer immobilization, PEG blocking, H5N1 binding (2^3 HAU) and signal amplification with $[\text{Fe}(\text{CN})_6]^{3-/4-}$ as a redox probe in the frequency range from 1 Hz to 1 MHz.

The result indicated that the developed impedance biosensor with specific aptamer was feasible for detection of AIVs. The result also demonstrated that TCA+NPApt

(a conjugation of aptamer, gold nanoparticles and thiocyanuric acid) could be used as an amplifier for

further amplification of the binding reaction between the aptamer and target AIV.

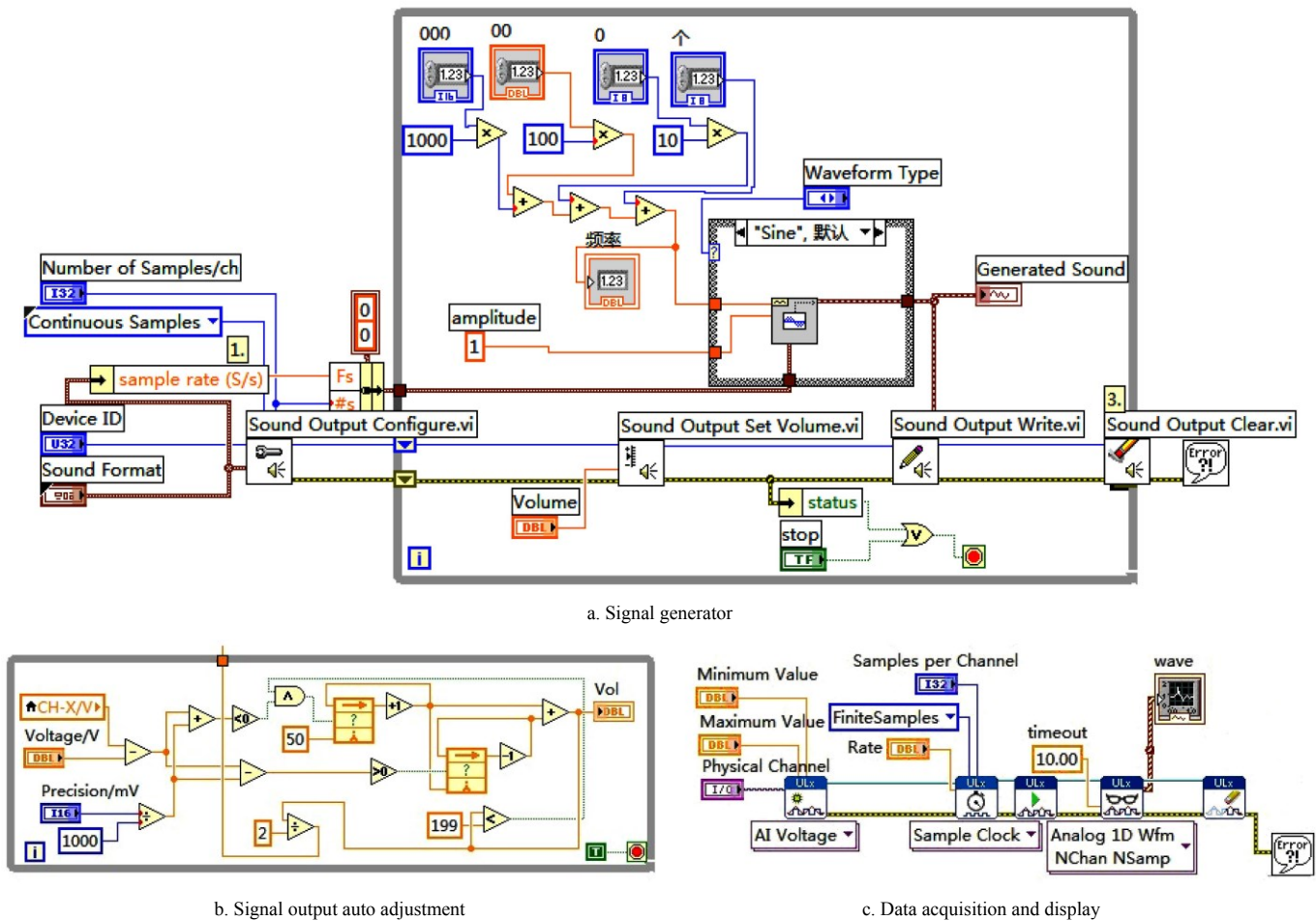


Figure 4 LabVIEW Program for the impedance biosensing system

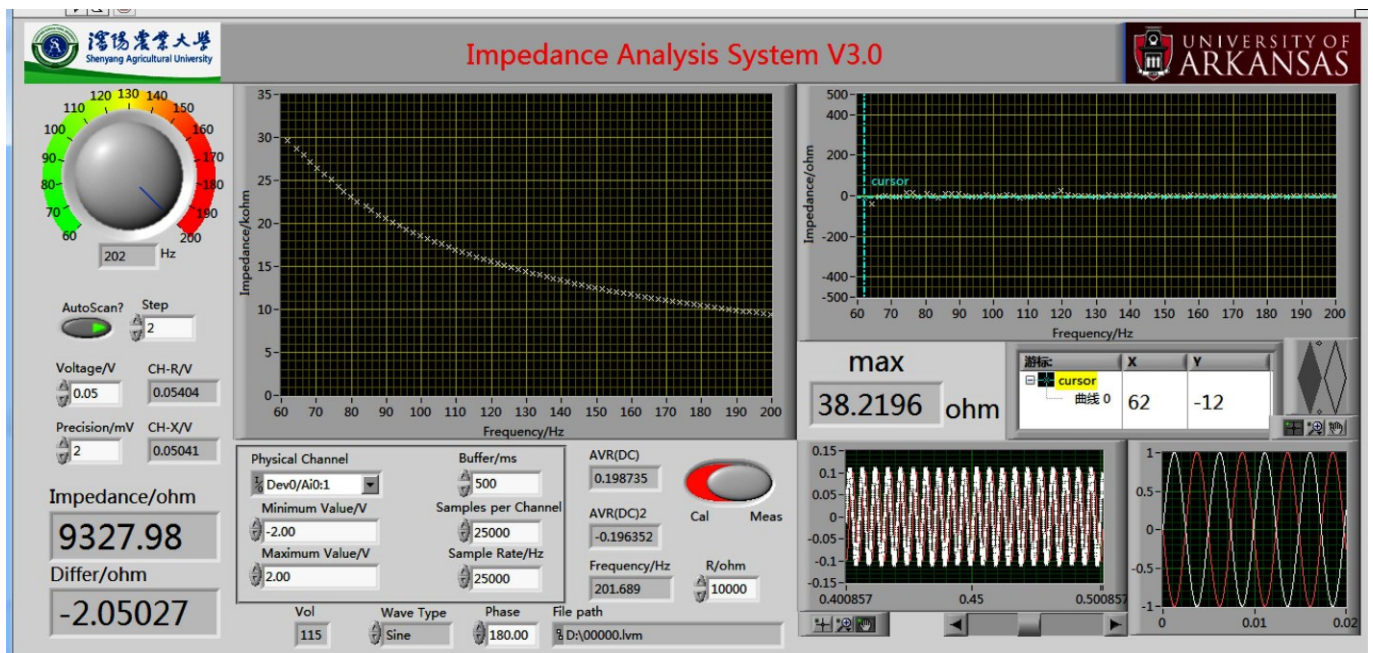


Figure 5 VI front panel for impedance measurement using LabVIEW

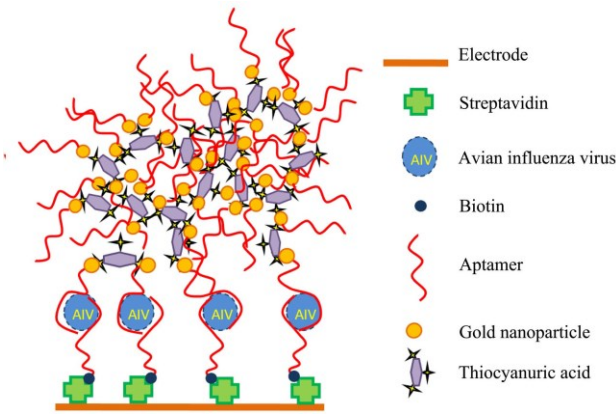


Figure 6 Principle of the microelectrode array based impedance biosensor for detection of AIVs

3.3 Calibration of impedance measurement

In order to check the detection accuracy of the developed system, the performance of solid circuit was tested by detection of solid capacity under different frequency and then in comparison with calculation. The result is listed in Table 1. After measuring the impedance of constant capacitor and its capacitance, it demonstrated that the difference of capacitance calculated under different frequencies was not significant, with an error less than 5%. The precision of the difference value was tested. The result was very close to the true value, when the sample period was setup to 1 min. As shown in Figure 5, the maximum error in the whole range configured was less than 50 Ω.

Table 1 Results of tests on solid capacity

F/Hz	V ₁ /V	V ₂ /V	Z _c /Ω	C _U /F	Err/%
10	0.169	0.961	10 713 159.76	9.33431E-08	-1.0
20	0.333	0.914	10 342 198.2	9.66912E-08	2.5
30	0.455	0.862	10 707 745.05	9.33903E-08	-1.0
40	0.566	0.788	10 491 816.25	9.53124E-08	1.0
50	0.663	0.71	10 087 782.81	9.91298E-08	5.1
60	0.72	0.671	10 534 700.00	9.49244E-08	0.6
70	0.776	0.611	10 383 850.52	9.63034E-08	2.1
80	0.811	0.564	10 481 637.48	9.54049E-08	1.1
90	0.834	0.53	10 775 395.68	9.2804E-08	-1.6
100	0.866	0.482	10 486 004.62	9.53652E-08	1.1
200	0.956	0.273	10 760 083.68	9.29361E-08	-1.5
300	0.98	0.186	10 727 265.31	9.32204E-08	-1.2
400	0.984	0.142	10 875 121.95	9.1953E-08	-2.5
500	0.985	0.112	10 7110 65.99	9.33614E-08	-1.0
600	0.996	0.097	11 008 915.66	9.08355E-08	-3.7

In addition, the measured impedance by the developed biosensor was compared with that by an impedance analyzer (BAS, IM6, West Lafayette, IN) and the result (Figure 8) indicated that both curves matched

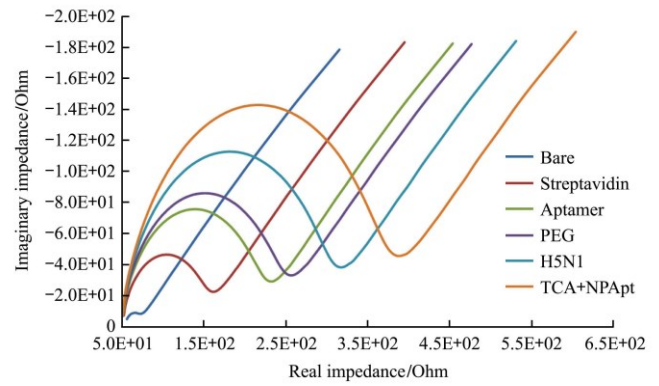


Figure 7 Typical Nyquist spectra of the biosensor surface modification, AIV H5N1 capture and signal amplification

well in the range of frequencies from 50 Hz to 5000 Hz with a correlation coefficient of 0.93. This system could accurately control the frequency and amplitude of the excitation signal. The accuracy of the system could be further enhanced if a DAQ with more bits is selected, the interference is better shielded, and/or the algorithm is optimized. Figure 8 shows that the system has a large error at low frequency, but the fitting effect is particularly good when the frequency exceeds 50 Hz. In practical applications, there are very few cases of lower than 50 Hz, such as the range of the frequency bands used in this study is 60-200 Hz.

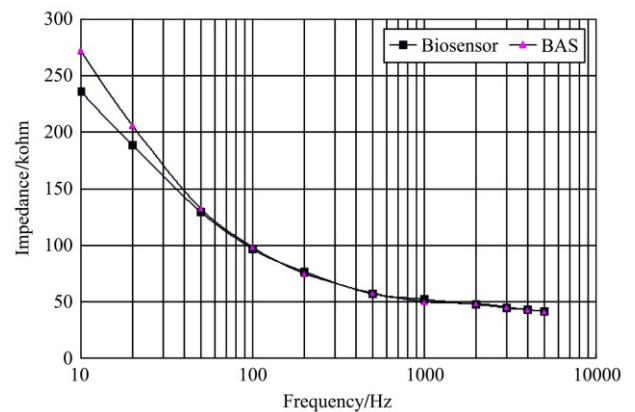


Figure 8 Comparison of impedance measurement between BAS impedance analyzer and the biosensor

3.4 Repeatability of impedance measurement

Two groups of impedance measurement tests were conducted using the same microelectrode with two methods and their results were compared. The impedance was measured in the presence of 10 mM [Fe(CN)₆]^{3-/4-} (1:1) mixture in PBS (pH7.4) as a redox probe in the frequency range from 50 Hz to 225 Hz with an amplitude of 5 mV. Bode (impedance and phase vs

frequency) charts are shown in Figure 9. IM6 could only provide 6 data points between 60 Hz to 200 Hz while the biosensing system can collect 70 data points with 2 Hz each step though program. Every step can be defined in the system.

Because the surface microelectrodes changed after each test, the measured impedance decreased in the repeated tests as expected. The results showed that the difference between the impedance values measured by IM6 (test No.1 and No.3) and IBS (test No.2 and No.4) increased as the increase of frequency. But the impedance values measured by the same method, either IBS or IM6, followed the curves in parallel, which indicates the good repeatability of impedance measurement in case of the change of the microelectrode surface. In Figure 9, the curves are approximately in parallel for the same method because the impedance of the sample gradually decreases as time goes by. It is worth mentioning that the frequency is scanned descending order by IM6, but increasing by IBS, therefore, the curves for different methods are not completely in parallel.

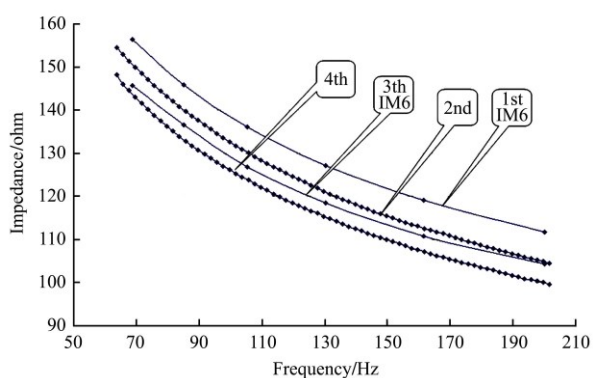


Figure 9 Comparison of impedance measurements between the biosensing system (IBS) and BAS impedance analyzer (IM6) using the same microelectrode

4 Conclusions

An impedance biosensing system was successfully designed in this research as a compact, portable instrument with the sensitivity and specificity for on-site or in-field rapid screening of multiple AIVs in poultry samples. The results showed that this portable virtual instrument based impedance analyzer has a high accuracy and an acceptable repeatability. Calibration algorithm was optimized for this virtual instrument based on the

comparison with the results of IM6. The measurement error was limited less than 5%.

The developed impedance biosensing system provided a novel platform for development of biosensing instruments for in-field rapid detection of pathogenic viruses and bacteria in agriculture and food.

Acknowledgements

This research was supported by Arkansas Biosciences Institute (ABI).

[References]

- [1] WHO, http://www.who.int/influenza/human_animal_interface/EN_GIP_20141204CumulativeNumberH5N1cases.pdf, Accessed on [2014-12-04].
- [2] WHO, Overview of the emergence and characteristics of the avian influenza A (H7N9) virus. May 31, 2013.
- [3] WHO, Influenza research at the human and animal interface. Report of a WHO working group. September 21-22, 2006, Geneva, Switzerland.
- [4] Bai H, Wang R, Hargis B, Lu H, Li Y. A SPR aptasensor for detection of avian influenza virus H5N1. *Sensors*, 2012; 12: 12506-12518.
- [5] Wang R, Li Y. Hydrogel based QCM aptasensor for detection of avian influenza virus. *Biosens. Bioelectron.*, 2013; 42: 148-155.
- [6] Zhang Y, Deng Z, Yue J, Tang F, Wei Q. Using cadmium telluride quantum dots as a proton flux sensor and applying to detect H9 avian influenza virus. *Anal. Biochem.*, 2007; 364: 122-127.
- [7] Xu J, Suarez D, Gottfried D. Detection of avian influenza virus using and interferometric biosensor. *Anal. Bioanal. Chem.*, 2007; 389: 1193-1199.
- [8] Qi C, Tian X, Chen S, Yan J, Cao Z, Tian K, et al. Detection of avian influenza virus subtype H5 using biosensor based on imaging ellipsometry. *Biosens. Bioelectron.*, 2012; 25: 456-460.
- [9] Lai W A, Lin C H, Y. S. Yang, M. S. Lu. Ultrasensitive and label-free detection of pathogenic avian influenza DNA by using CMOS impedimetric sensors. *Biosens. Bioelectron.*, 2010; 35: 1530-1534.
- [10] Bolis S D, Charalambous P C, Efstathiou C E, Mantzila A G, Malamou C A, Prodromidis M I. Monitoring of the avidin-biotinylated dextran interaction on Au- and Ti/TiO₂-electrode surfaces using a charge integrating device. *Sens. Actuat. B*, 2006; 114: 47-57.
- [11] Wang R, Zhao J, Jiang T, Kwon Y M, Lu H, Jiao P, et al. Selection and characterization of DNA aptamers for use in

- detection of avian influenza virus H5N1. *J. Virol. Meths.*, 2013; 189: 362–369.
- [12] Lum J, Wang R, Lassiter K, Srinivasan B, Abi-Ghanem D, Berghman, et al. Rapid detection of avian influenza H5N1 virus using impedance measurement of immuno-reaction coupled with RBC amplification. *Biosens. Bioelectron.*, 2011; 38(1): 67–73.
- [13] Ram Y, Yoetz-Kopelman T, Dror Y, Freeman A, Shacham-Diamand Y. Impact of molecular surface charge on biosensing by electrochemical impedance spectroscopy. *Electrochimica Acta*, 2016; 200: 161–167.
- [14] Lu Y, Guo Z, Song J J, Huang Q A, Zhu S W, Huang X J, et al. Tunable nanogap devices for ultra-sensitive electrochemical impedance biosensing. *Analytica Chimica Acta*, 2016; 905: 58–65.
- [15] Wu C C, Huang W C, Hu C C. An ultrasensitive label-free electrochemical impedimetric DNA biosensing chip integrated with a DC-biased AC electro osmotic vortex. *Sensors and Actuators B: Chemical*, 2015; 209: 61–68.
- [16] Chen Y, Wang J, Liu Z M. Graphene and Its Derivative-based Biosensing Systems. *Journal of Analytical Chemistry*, 2012; 40(11): 1772–1779.
- [17] Cao X D, Ye Y K, Liu S Q. Gold nanoparticle-based signal amplification for biosensing. *Analytical Biochemistry*, 2011; 417: 1–16.
- [18] Heileman K, Daoud J, Tabrizian M. Dielectric spectroscopy as a viable biosensing tool for cell and tissue characterization and analysis. *Biosensors and Bioelectronics*, 2013; 49: 348–359.
- [19] Kim S G, Lee H J, Lee J H, Jung H I, Yook J G. A highly sensitive and label free biosensing platform for wireless sensor node system. *Biosensors and Bioelectronics*, 2013; 50: 362–367.
- [20] Bonanni A, Loo A H, Pumera M. Graphene for impedimetric biosensing. *TrAC Trends in Analytical Chemistry*, 2012; 37: 12–21.
- [21] Voiculescu I, Nordin A N. Acoustic wave based MEMS devices for biosensing applications. *Biosensors and Bioelectronics*, 2012; 33: 1–9.
- [22] Kashefi-Kheyraadi L, Mehrgardi M A. Design and construction of a label free aptasensor for electrochemical detection of sodium diclofenac. *Biosensors and Bioelectronics*, 2012; 33: 184–189.